

Article

Effect of Y Alloying on Microstructure and Mechanical Properties of AZ61 Magnesium Alloy Sheets Applied as 3C Electronic Product Shells

Jian Wang ^{1,2,3}, Zheng Chang ³, Boyu Liu ³ , Yongbing Li ^{1,2}, Yan Sun ^{1,2} and Hongxiang Li ^{3,*} 

¹ State Key Laboratory for Advanced Forming Technology and Equipment, China Academy of Machinery Science and Technology, Beijing 100044, China

² Beijing National Innovation Institute Lightweight Ltd., Beijing 100083, China

³ State Key Laboratory for Advanced Metals and Materials, University of Science and Technology Beijing, Beijing 100083, China

* Correspondence: hxli@skl.ustb.edu.cn

Abstract: AZ61 magnesium alloy sheets can be applied as 3C (computer, communication, and consumer) electronic product shells. However, due to their poor plasticity and relatively low strength, the application of AZ61 alloy sheets is limited. The composition modification of AZ61, especially rare earth element alloying, is a good choice to improve the strength and plasticity of AZ61 alloy sheets. In this paper, the strength and plasticity of AZ61 sheets with different contents of Y were studied in detail. We found that the addition of 0.9 wt.% of Y not only improved the strength, but also significantly enhanced the plasticity. As a result, the yield strength of AZ61 increased from 167 MPa to 186 MPa, and the elongation increased from 9.5% to 18%. The reasons can be explained as follows: the Al₂Y phase formed by adding Y consumed a large amount of the Al element, thus avoiding the formation of the brittle phases Al₃Mn₅ and resulting in the improved mechanical properties of the sheets. At the same time, the weakened texture and dispersed grain orientation also effectively improved the plasticity of the sheets. This study will provide a good solution to improve the strength and plasticity of AZ61 sheets without significantly increasing the production cost.

Keywords: AZ61 magnesium alloy sheets; mechanical properties; Y alloying; precipitates; strengthening mechanism



Citation: Wang, J.; Chang, Z.; Liu, B.; Li, Y.; Sun, Y.; Li, H. Effect of Y Alloying on Microstructure and Mechanical Properties of AZ61 Magnesium Alloy Sheets Applied as 3C Electronic Product Shells. *Crystals* **2022**, *12*, 1643. <https://doi.org/10.3390/cryst12111643>

Academic Editors: Erdem Karakulak and Huseyin Sevik

Received: 22 October 2022

Accepted: 9 November 2022

Published: 16 November 2022

Publisher's Note: MDPI stays neutral with regard to jurisdictional claims in published maps and institutional affiliations.



Copyright: © 2022 by the authors. Licensee MDPI, Basel, Switzerland. This article is an open access article distributed under the terms and conditions of the Creative Commons Attribution (CC BY) license (<https://creativecommons.org/licenses/by/4.0/>).

1. Introduction

With the development of Internet technology and the maturity of 5G technology, the characteristics of low latency and high network speed are more prominent. The popularity of cloud services will be greatly improved, which is inseparable from the application of notebook computers and mobile phones. Due to its low density, high specific strength, high damping characteristics, and good recyclability, magnesium alloy has become the preferred alloy for lightweight design and energy saving for 3C electronic products. The common magnesium alloy sheets can be generally divided into four categories: the Mg–Al series, Mg–Zn series, Mg–Li series, and Mg–RE series alloys [1–5]. However, the Mg–RE alloy is limited by the expensive cost of the rare earth element, and the Mg–Li alloy needs to be melted in a vacuum environment, which undoubtedly greatly increases the cost and processing complexity. Although the Mg–Zn alloy exhibits good plasticity, it is difficult to meet the requirements of 3C electronic products due to its relatively low strength. Due to the outstanding mechanical properties and good formability, the most common magnesium alloy applied for 3C electronic products is the Mg–Al series alloy, such as AZ31, AZ61, AZ80, AZ91, and so on and AZ31 occupies the mainstream market for thin magnesium alloy sheets. However, due to the low alloying of AZ31 alloys, its strength is still lower, and its formability is also not enough to meet the requirement of more advanced magnesium

alloy sheets. On the other hand, the AZ80 and AZ91 alloys have poor plasticity due to high alloying contents, which also makes it difficult to be applied as 3C electronic products. The AZ61 alloy has a medium alloying level, and its mechanical properties are also relatively high, thereby exhibiting further development prospects for 3C electronic products.

Processing modification and alloying modification are two effective methods in improving the strength and plasticity of magnesium alloy sheets. As for the preparation, the existing method usually faces the problem of increasing plasticity and decreasing strength at the same time. The mechanical properties of the undeformed Y-alloyed AZ61 cast plates are very poor, and the elongation of AZ61 with 1.2 wt.% of Y is less than 6%, and the tensile strength is less than 200 MPa [6]. To improve the plasticity while maintaining the higher strength, it is necessary to develop new preparation methods to solve the problem. Some asymmetric deformation preparation methods, such as equal-channel angular pressing (ECAP) and continuous bending (CB), can not only refine the grains and improve the strength, but also change the grain orientation to improve the plasticity [7–11]. For example, Huo et al. [10] introduced cyclic shear strain through bidirectional cyclic bending, which can make AZ61 sheets exhibit an elongation of more than 30% while maintaining the tensile strength of more than 270 MPa. Through the process of combining ECAP and electropulsing treatment, Shan et al. [12] developed the new AZ61 alloy sheets, and the tensile strength of the sheets can reach more than 400 MPa while maintaining the elongation of more than 17%. However, the improvement of these preparation methods is limited by the equipment, such as ECAP, electropulsing treatment, and bidirectional cyclic bending. Generally, the pieces of equipment used in these processes are too complex, and they are not adaptable in the large-scale production of magnesium alloy sheets [13–15].

In terms of alloying, rare earth (RE) element alloying is a better choice to improve the plasticity of magnesium alloy sheets. RE elements can not only retain the strength of sheets by refining grains and generating precipitation, but also improve the plasticity of sheets by coordinating grain orientation [16–18]. Zhao et al. [19] found that adding the Gd element can improve the plasticity of the magnesium alloy sheets. Because the texture strength was reduced from 9.62 to 7.82, the plasticity in the transvers direction (TD) and extrusion direction (ED) were improved, and the elongation in ED could reach 34.6%. Other scholars [20] have also shown that the addition of the Y element makes the grain orientation of Mg–Y alloy deflect, thus enhancing the mechanical properties of magnesium alloy sheets. When only 0.5 wt.% of Y is added, the tensile strength is increased by nearly 20 MPa, and the elongation is increased by 3%. When the content of Y is further increased to 5 wt.%, the tensile strength is further increased by 60 MPa, and the elongation is increased by 11%. Therefore, it can be concluded that the addition of the RE elements can perhaps improve the plasticity of magnesium alloy sheets while retaining their high strength. Thus, the alloying modification of the RE elements is a more suitable method to improve the properties of the AZ61 magnesium alloy sheet. The addition of Nd and Gd in the AZ61 alloys can improve the plasticity, but the strength decreases obviously [21–24]. However, when we searched the corresponding references, we found that systematic investigations were lacking until now on the role of Y alloying in AZ61 alloy sheets [25–29]. Based on the above aim, in this study, AZ61 alloy sheets with different contents of the Y element were prepared by the conventional method combining the extrusion and rolling techniques. The effect of microalloying of the Y element on the microstructure and properties of AZ61 alloy sheets was studied systematically. In addition, the microstructure evolution rule after adding the Y element and the mechanism on improving the strength and plasticity of AZ61 sheets was explored in detail.

2. Materials and Methods

In this paper, the resistance furnace was used to melt the AZ61-modified alloy, and the metal melt was cast into the steel mold to obtain the required ingots with a length of 90 mm and a diameter of 90 mm. The homogenization was carried out at 400 °C for 16 h, and then air cooling was carried out. Before extrusion, the ingots and mold were all

preheated to 400 °C. The extrusion temperature was 400 °C, and the extrusion ratio was 21:1 for the AZ61-modified alloy ingots. The alloy sheets with a thickness of 3 mm were obtained by extrusion. After the sheets were preheated to 400 °C × 30 min, the alloy sheets were rolled, and the reduction in each pass was 10–15%. After each pass of rolling, the alloy sheets were returned to the furnace for heating, and the temperature was kept at 400 °C for 10 min. Finally, the alloy sheets with a thickness of 1 mm were obtained. The sheets were put into the heat treatment furnace for 300 °C × 40 min annealing. The schematic diagram showing the preparation process employed in the present study is shown in Figure 1.

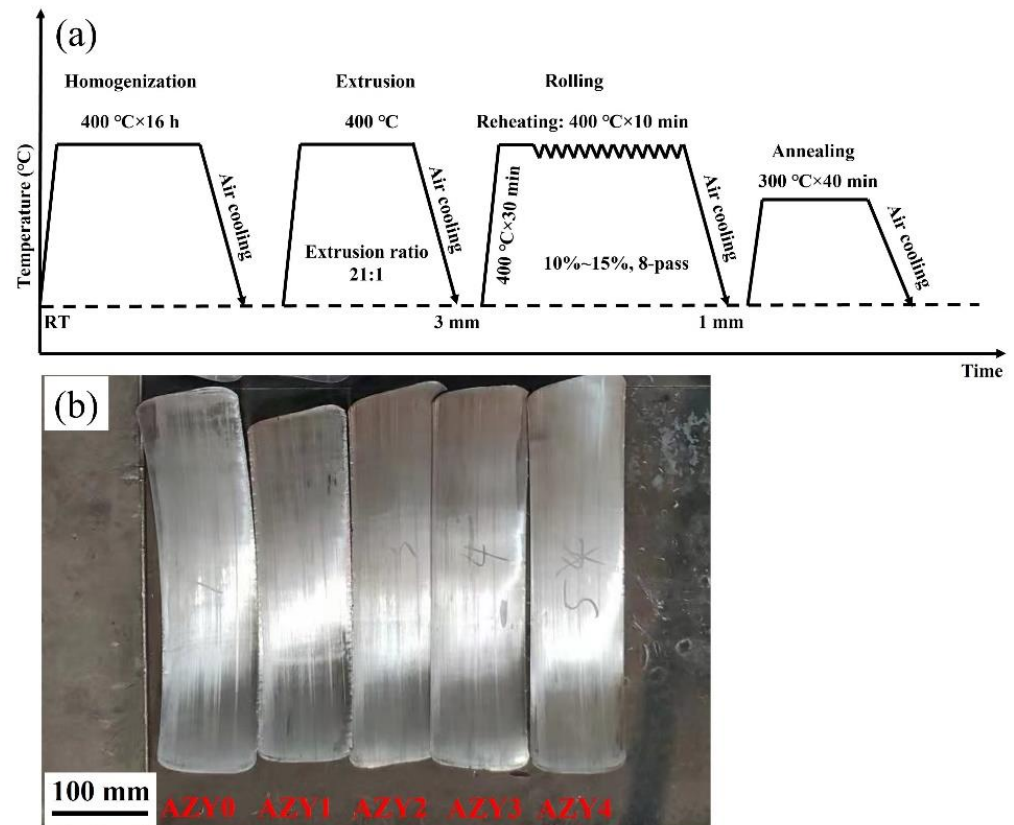


Figure 1. The schematic diagram showing the preparation process employed in the present study: (a) Schematic diagram; (b) Final rolled sheets.

Five groups of samples with the compositions of AZ61-xY ($x = 0, 0.3, 0.6, 0.9, 1.5$ wt.%) were prepared in this experiment and numbered AZY0, AZY1, AZY2, AZY3, and AZY4 according to the above compositions, respectively. X-ray fluorescence spectrometer (XRF, MXP21VAHF, Japan) tests were carried out as shown in Table 1 for confirming the alloy composition. The microstructure was observed by optical microscope (OM, Carl Zeiss AG, Axio imager.A2m, German) and scanning electron microscope (SEM, Carl Zeiss AG, Zeiss supra55, German), respectively. The texture, grain orientation, and other microstructure data of the rolled sheets were collected and analyzed by electron backscatter diffraction (EBSD, Carl Zeiss AG, Zeiss supra55, German). The precipitated phases of the samples were observed by transmission electron microscope (TEM, FEI Company, TECNAI F20, American), and the TEM samples were prepared by ion milling method. A CMT4204 universal tensile testing machine (Mester, Shenzhen, China) was used to conduct tensile test on the samples, and three parallel samples were taken from each group to take the average value. The tensile tests were performed at room temperature, and the strain rate was 1 mm/min.

Table 1. Composition analysis of the AZ61 sheets with different Y contents (wt.%).

	Al	Zn	Mn	Y	Mg
AZY0	5.7	0.6	0.2		Bal.
AZY1	6.3	0.6	0.2	0.3	Bal.
AZY2	5.8	0.6	0.2	0.6	Bal.
AZY3	5.6	0.5	0.2	0.9	Bal.
AZY4	6.3	0.5	0.2	1.5	Bal.

3. Results

3.1. Microstructure

The OM metallographic images of the AZ61-modified rolled sheets are shown in Figure 2. For the AZY0, AZY1 and AZY2 sheets, the deformation grains dominated, which were arranged at an angle of 45° to the deformation direction (Figure 2a–c). Among them, the AZY0 grains were relatively fine (Figure 2a), and with the increase in Y content, the size of the grains further decreased (Figure 2b,c). When the content of Y was further increased above 0.9 wt.%, there were no longer deformation grains in the AZY3 and AZY4 sheets, but the equiaxed crystals were the main structure, and the number of precipitates in AZY3 and AZY4 were also increased significantly.

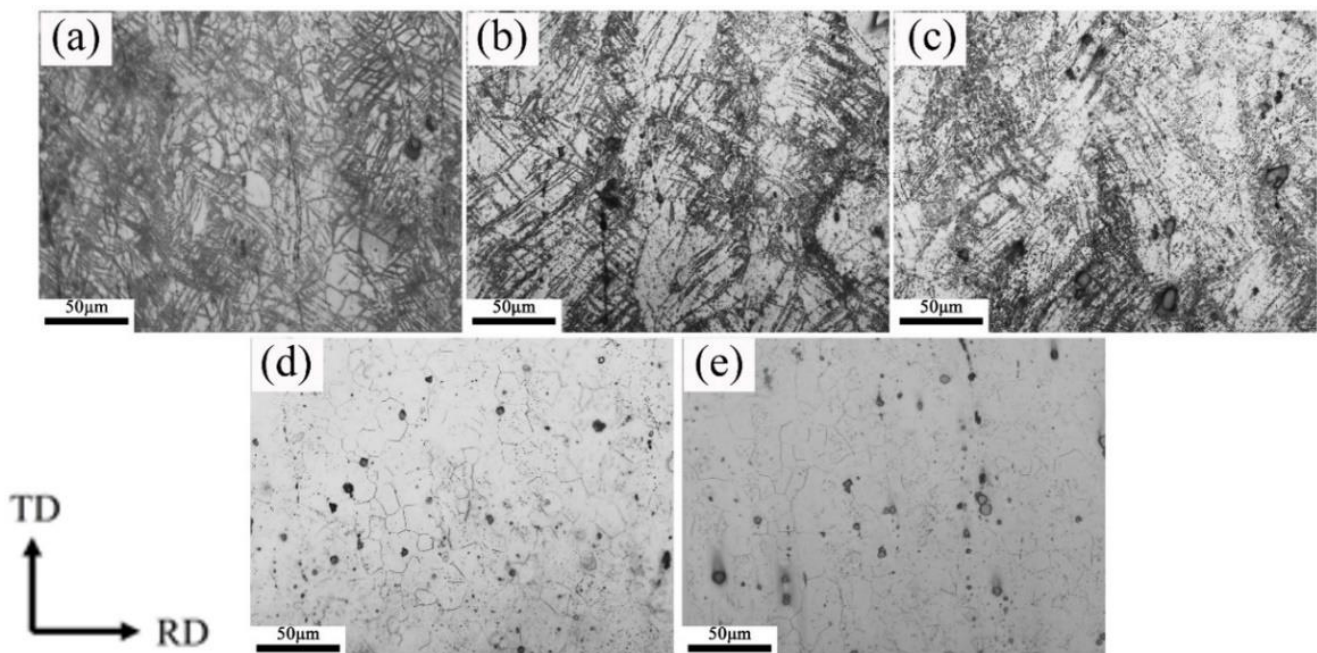


Figure 2. Optical microstructure of the rolled sheets with different Y contents: (a) AZY0; (b) AZY1; (c) AZY2; (d) AZY3; and (e) AZY4.

The SEM images of the AZ61-modified rolled sheets are shown in Figure 3. For the AZY0 alloy sheets, less precipitates could be observed, and the grains size was also smaller (Figure 3(a1)). However, for the AZY1 alloy sheets, the number of precipitates increased significantly, and dispersed spherical precipitates also appeared (Figure 3(b1)). However, when the content of the Y element continued to increase, the number of precipitates not only increased, but also large-sized precipitates could be observed (Figure 3(c1–e1)).

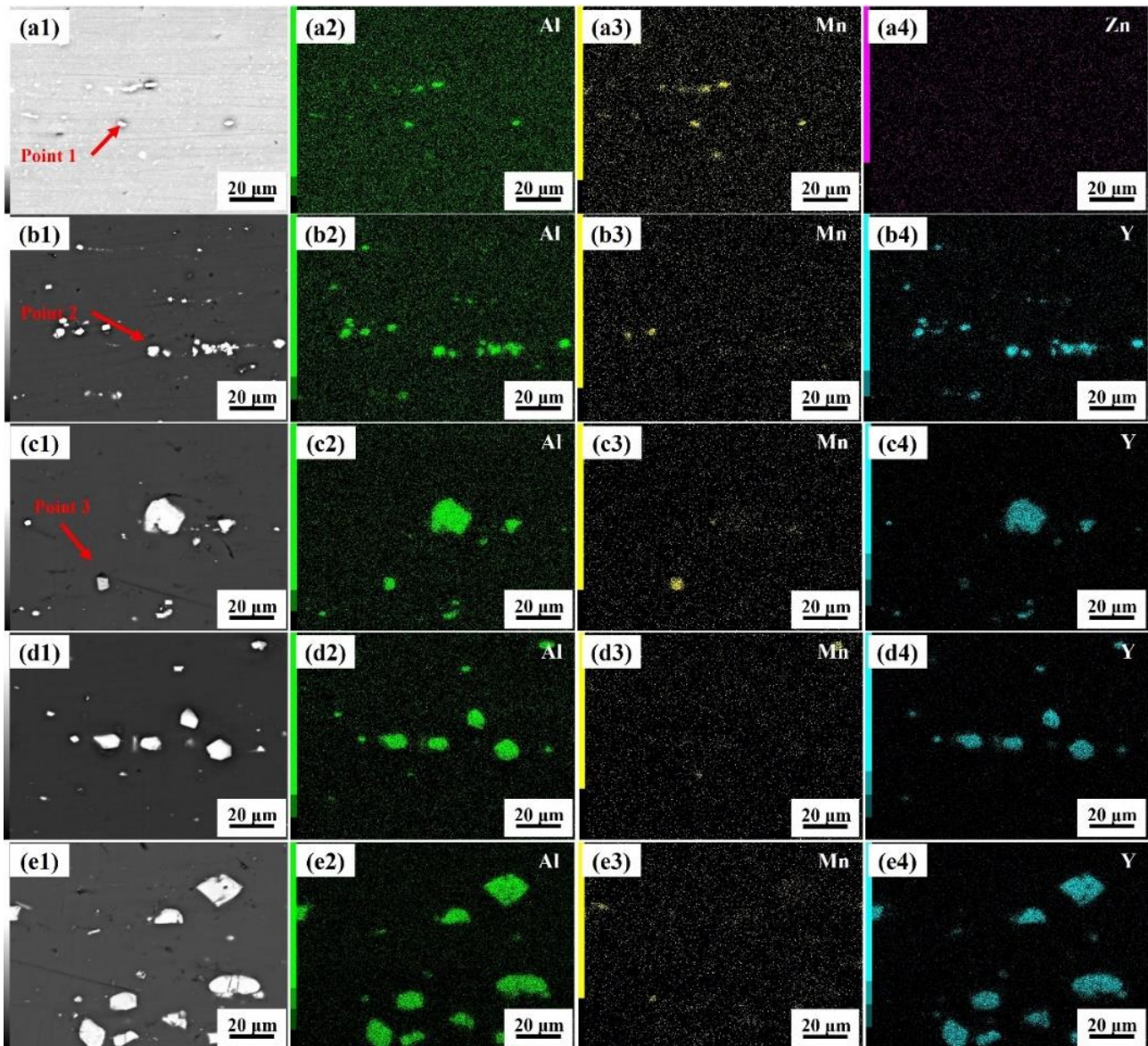


Figure 3. SEM images and EDS images of the rolled sheets with different Y contents: (a) AZY0; (b) AZY1; (c) AZY2; (d) AZY3; and (e) AZY4.

The EDS images of the AZ61-modified rolled sheets are shown in Figure 3. For the AZY0 alloy sheets, Zn was a uniformly solid solution in the matrix and did not participate in the formation of precipitates (Figure 3(a4)). The Al element and the Mn element could form Al–Mn precipitates (Figure 3(a2,a3)). According to Table 2, there were many small-sized Al_8Mn_5 precipitates (Point 1) in the AZY0 alloy sheets. Moreover, for the AZY1 and AZY2 alloy sheets, the Al–Y precipitates were mainly observed, and a small number of Al–Mn–Y precipitates were also precipitated (Figure 3(b1–c4)). In combination with Table 2, the Al–Y precipitates were mainly confirmed to be the Al_2Y phase (Point 2). After consulting the relevant literature and combining with the EDS analysis of Point 3, those small Al–Mn–Y precipitates could be confirmed to be the $\text{Al}_8\text{Mn}_4\text{Y}$ phase [30]. When the Y content continued to increase, the number of Al–Y precipitates in AZY3 and AZY4 continued to increase, but the number of Al–Mn–Y precipitates gradually decreased (Figure 3(d1–e4)).

Table 2. Test components of EDS points for the AZ61 sheets with different Y contents.

Point	Element	Atomic Conc. (at.%)	Weight Conc. (wt.%)
1	Mg	38.01	30.28
	Al	45.71	40.41
	Mn	16.28	29.31
2	Mg	8.80	4.62
	Al	58.83	34.29
	Mn	1.46	1.73
	Y	30.91	59.36
3	Mg	53.87	41.98
	Al	30.70	26.55
	Mn	11.50	20.25
	Y	3.94	11.22

The inverse pole figure (IPF) and pole figure (PF) of the rolled sheets with different Y contents are shown in Figure 4. After rolling, the grains were mainly equiaxed grains, and most of the grains showed a concentrated orientation with (0001) planes parallel to the rolled direction (RD) (Figure 4). Part of the black areas in the IPF were unrecognizable by the EBSD because the deformation was too large, resulting in serious grain breakage, which made the probe unrecognizable. When the content of Y was low, it could be seen from the PF that the AZY0 and AZY1 sheets all exhibited an obvious basal texture (Figure 4b,d). However, when the Y content increased to 0.6 wt.%, the texture of the AZY2 sheets changed into a bimodal texture, and the texture intensity also decreased from 16 of AZY0 to 13 of AZY2 (Figure 4f). When the Y content was further increased, the texture of the AZY3 and AZY4 sheets showed an obvious bimodal texture, but the texture intensity increased from 13 of AZY2 to 17 of AZY4 (Figure 4h,j).

The recrystallization statistics of the rolled sheets with different Y contents are shown in Figure 5. The recrystallization fraction of the AZY0 sheets was less than 60%. With the increase in Y content, the recrystallization fraction of AZY1 decreased to 61%. However, with a further increase in Y content, for the AZY2 alloy sheets with 0.6 wt.% of the Y element, the recrystallized grain fraction reached more than 70%, and the fraction of deformed grain also decreased significantly. For the AZY3 alloy sheets, the recrystallized grain fraction even reached 93%, and the deformed grain fraction decreased to 0.2%. With a further increase in Y content, the recrystallization fraction of the AZY4 alloy sheets decreased to 78%.

The TEM images of the rolled AZY0 and AZY3 alloy sheets are shown in Figure 6. There were circular precipitates in the AZY0 alloy with a size of 100–300 nm. According to the diffraction pattern, it could be confirmed that this circular precipitate was the $Mg_{17}Al_{12}$ phase (as shown in Figure 6a). When the structure was enlarged, in addition to $Mg_{17}Al_{12}$, there were other precipitates with a size between 5–30 nm. Because the precipitate was too small to be calibrated by the diffraction pattern, it could only be analyzed by EDS, which was confirmed to be the Al_8Mn_5 phase (as shown in Figure 6b). For the AZY3 alloy sheets, a large precipitate was precipitated. Because the precipitate was too thick, the diffraction pattern could not be obtained, but the precipitate was analyzed by EDS to be the Al_2Y phase (Figure 6c). On the other hand, for the rolled AZY3 alloy sheets, the sizes of $Mg_{17}Al_{12}$ and Al_8Mn_5 decreased significantly (Figure 6d).

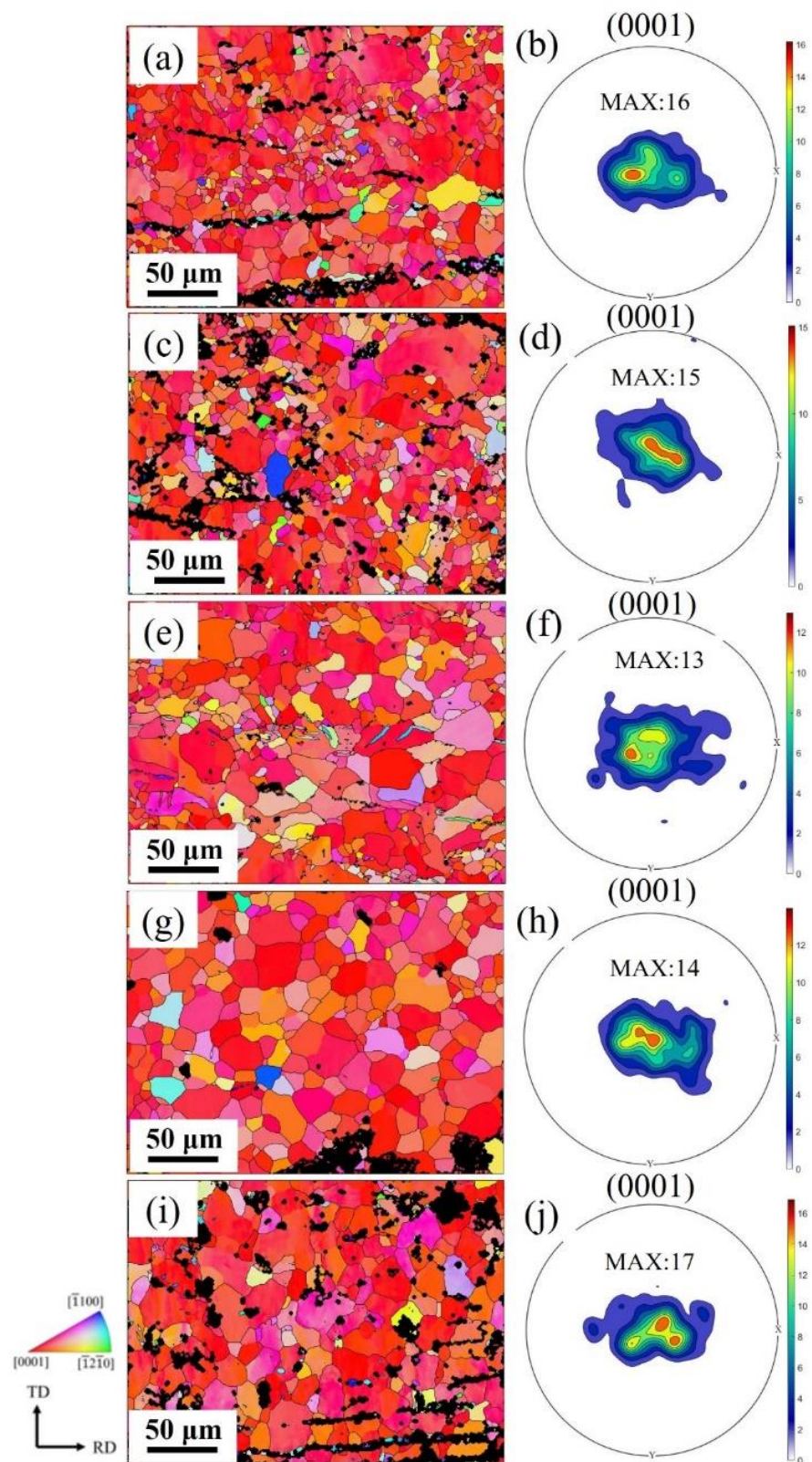


Figure 4. The IPF and the corresponding {0001} pole figures of the rolled sheets with different Y contents: (a,b) AZY0; (c,d) AZY1; (e,f) AZY2; (g,h) AZY3; and (i,j) AZY4.

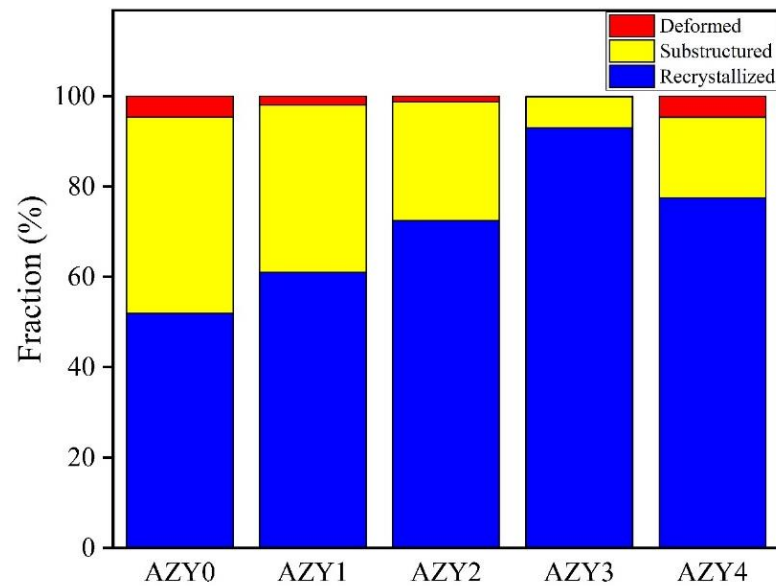


Figure 5. Statistical diagram of grain recrystallization for the rolled sheets with different Y contents.

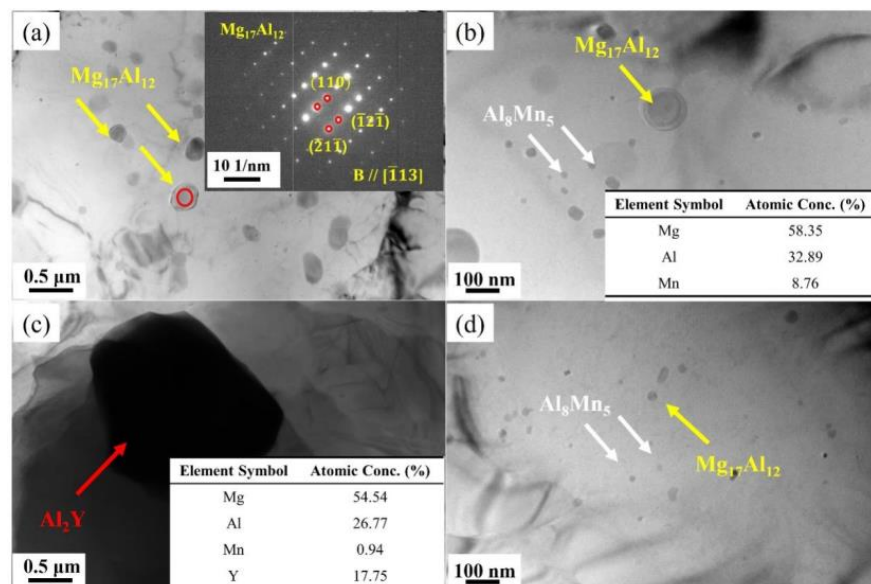


Figure 6. TEM images of the rolled sheets with different Y contents: (a,b) AZY0; (c,d) AZY3.

3.2. Mechanical Properties

Figure 7 shows the mechanical properties of the rolled sheets with different Y contents. The tensile strength and yield strength of the rolled sheets with different Y contents showed a consistent trend. So, with the increase in the content of the Y element, the tensile strength increased greatly and then decreased slightly (Figure 7a). However, the tensile strength of the sheets after adding Y was generally higher than that of AZ61 (AZY0). The tensile strength and yield strength of the AZY1 were the largest, reaching 301 MPa and 206 MPa, respectively, and the elongation reached 12% (as shown in Figure 7b). The change of elongation of the sheets is shown in Figure 7b. With the increase in Y content, the elongation of the sheets tended to increase first and then decrease. When the content of the Y element was 0.9% (AZY3), the elongation of the sheets had an obvious increase from 12% of AZY2 to 18% of AZY3, but the yield strength and tensile strength decreased to 186 MPa and 271 MPa, respectively.

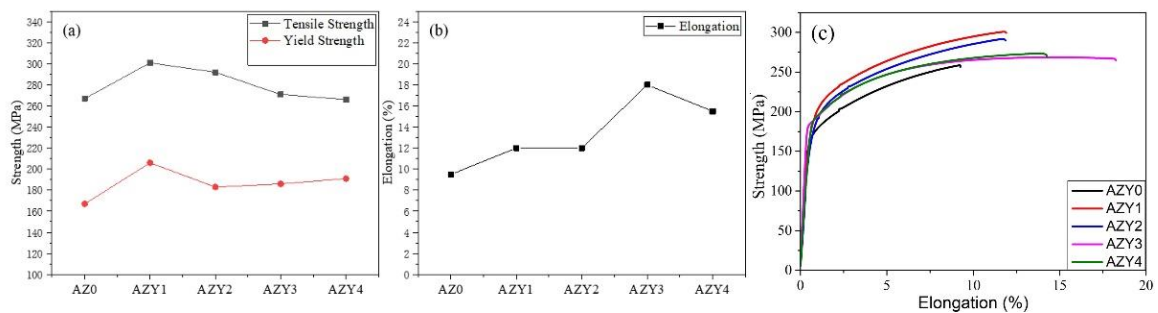


Figure 7. Mechanical properties of the rolled sheets with different Y contents: (a) tensile strength and yield strength of sheets; (b) elongation of sheets; and (c) stress–strain curve.

Figure 8 is the tensile fracture morphology of the rolled sheets with different Y contents. For the AZ61 alloy sheets (AZY0), many river-like cleavage planes and cleavage steps could be observed from the fracture surface. The fracture forms belonged to quasi-cleavage fractures and shear fractures, which are typical brittle fractures. That is why the AZY0 alloy was poor in plasticity. On the fracture surface of the AZY1 and AZY2 alloys, in addition to a small number of shallow dimples, some tear ribs and cleavage planes with river-like patterns could be observed, which belonged to the mixed fractures, and so the plasticity was improved. On the other hand, many dimples and ductile tearing edges on the fracture surface of the AZY3 and AZY4 alloys could be seen, and there were almost no cleavage planes, indicating that the plasticity of these alloys was excellent. The tensile fracture images matched the mechanical properties of the rolled sheets with the different Y contents very well.

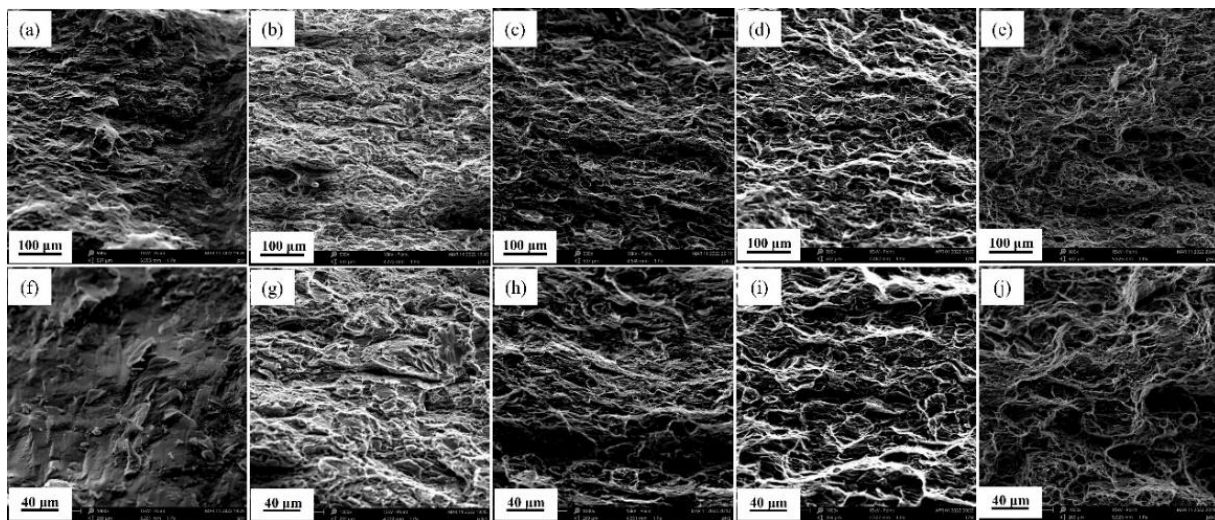


Figure 8. Tensile fracture images of the rolled sheets with different Y contents: (a,f) AZY0; (b,g) AZY1; (c,h) AZY2; (d,i) AZY3; and (e,j) AZY4.

4. Discussion

Figure 2 shows that the microstructures of the alloy sheets with different Y contents after deformation were completely different because the magnesium alloys had fewer slip systems due to their hexagonal close-packed (HCP) structure, and generally they could only be plastically deformed by the actuation of the basal slip system. When Y was not added to the AZ61 alloy (Figure 2a) or only a small amount of Y was added (Figure 2b,c), the deformation was difficult especially when the deformation amount was large. This also produced many deformed grains along the RD. When the added Y content was high, the addition of Y promoted a transformation of the texture type and a reduction in texture strength (Figure 4f,h,j). The deformation grains were replaced by twins and fine

equiaxed crystals in the alloys (Figure 2d,e). In addition, the dynamic recrystallization prevented the alloy sheets from cracking during large deformation process, because through recrystallization nucleation and growth, the alloy sheets released the deformation energy stored in the rolling process.

Because the rolled sheets were prepared by large deformation rolling, no $Mg_{17}Al_{12}$ phase with the large size was found in the AZ61-modified rolled sheets (Figure 3(a1)). The difficulty of forming intermetallic compounds depended on the heat of the alloy formation. When the heat of the formation of the alloy was negative, and the smaller the value was, the easier and stabler the phase was. Referring to the literature, the heat of formation of the $Mg_{17}Al_{12}$ and Al_2Y alloys was -287.6124 KJ/mol and -442.3954 KJ/mol, respectively [31]. This indicated that Al_2Y was easier to be formed and stabler. When the Al and Y elements reacted to form Al_2Y , the content of the Al element in the matrix was reduced. Because the consumption of Al increased, the number and size of the $Mg_{17}Al_{12}$ and Al_8Mn_5 phases tended to be decreased.

The grain orientation of the sheets was mainly concentrated in the (0001) plane parallel to the RD, and the grain size was significantly reduced with the addition of the Y element. The common deformation mechanisms of magnesium alloys are basal slip and twins, which is also the reason for the formation of a basal texture. There were many black areas in AZY0 and AZY1 (Figure 4a,c) because many grains were broken during the large deformation rolling. There were a few black areas in AZY2 and AZY3 (Figure 4e,g), which was due to the production of many twins and recrystallization grains. Twins and recrystallization grains can change the orientation of the crystals, releasing the stress concentration, which avoids the breakage of the grains while the deformation occurs. Since the large size precipitates increased (Figure 3(e1)), which prevented the grain deformation during rolling, the black area in AZY4 increased again (Figure 4i).

According to EBSD data statistics, the average grain size of each alloy was determined to be 4.97, 4.25, 4.16, 3.88, and 3.52 μm for the AZY0, AZY1, AZY2, AZY3, and AZY4 alloy sheets, respectively. With the increase in Y content, the average size of the grains decreased. When the content of the Y element was 0.5%, the grain shape of AZY3 was very uniform, and the size difference between grains was small. Due to the increase in Y content from 0 to 0.9 wt.%, the Al–Y phase generated inhibited the growth of the recrystallized grains and refined the recrystallized grains. However, with the further increase in Y content to 1.5 wt.%, although the grain size was reduced, many of the precipitates generated hindered the grain growth, which led to an uneven grain shape and a decrease in the mechanical properties. Uneven grains and many precipitated phases resulted in the elongation of the sheets decreasing from 18% to 15.5%.

As shown in Figure 6b,d, the large consumption of the Al elements by the generation of Al_2Y led to the reduction in Al elements that could participate in the generation of Al_8Mn_5 and $Mg_{17}Al_{12}$, thus reducing the size and quantity of Al_8Mn_5 and $Mg_{17}Al_{12}$ in the AZY3 sheet. Small-sized precipitates could retain the strength of the sheets. It is for this reason that the strength of AZY1–AZY4 was better than the strength of AZY0.

Figure 7 shows that AZY1 with 0.3 wt.% of Y had the highest yield strength and tensile strength, reaching 206 MPa and 301 MPa, respectively, as the result of many small-sized Al_2Y precipitates and a high texture strength of basal texture. The addition of a small amount of Y element did not change the structure of the alloy greatly, and the elongation of the AZY1 sheets was only 12%. In the AZY1 sheets, the texture was still the basal texture (Figure 4d). The basal texture was conducive to improving the strength of the sheet, but not conducive to improving the elongation. Compared with AZY1, the strength of AZY2 decreased by about 20 MPa, but the elongation remained unchanged at 12%. The reason for the change of properties was that the basal texture had begun to change to a bimodal texture, and the strength provided by the centralized orientation was dispersed by the multidirectional grain orientation, leading to a decrease in strength. At this time, there were still many deformed grains as shown in Figures 1c and 4c, which made the elongation remain at 12%. Regarding other research of AZ61 sheets with 0.9 wt.% of Y, the elongation

increased from 18.1% to 20% in Fang's research, so the increase amount was only 2% [32]. In this study, the elongation of AZY3 (0.9 wt.% Y) increased from 9% to 18%, an increase of 9%. The obvious bimodal texture of the AZY3 sheets could be observed as shown in Figure 4h, and the recrystallized grain fraction also reached 93% (as shown in Figure 5). These factors increased the elongation of the alloy, which could reach 18%. The bimodal texture made the strength of the AZY2 sheets lower than AZY1, but the strength of AZY2 was higher than AZY0 due to the reduction in grain size, the increase in precipitation phase, and the increase in recrystallization grains. However, with the further increase in Y content to 1.5 wt.%, the formation of many large-sized Al_2Y precipitates inhibited the deformation and recrystallization growth of grains in the rolling process, which led to grain breakage, uneven grain size, and reduction in the number of recrystallized grains in the AZY4 sheets. These factors reduced the elongation of AZY4 to 15.5%.

5. Conclusions

The effect of Y alloying on the microstructure and mechanical properties of the AZ61-modified rolled sheets were systematically investigated. The following main conclusions could be drawn:

- (1) The addition of Y could form the Al_2Y phase and effectively promoted the occurrence of recrystallization, so that many parallel or interlaced deformation grains in the AZ61 magnesium alloy sheet gradually changed into the equiaxed crystal structures and completed the macroplastic deformation of the alloy.
- (2) The addition of Y could weaken the texture and changed the texture type and made the concentrated grain orientation dispersed. The weakened bimodal texture improved the elongation significantly in 0.9 wt.% of the Y-modified AZ61 sheets.
- (3) The main precipitate phase of the Y-alloying AZ61 sheets was Al_2Y . Due to the large consumption of the Mn and Al elements, there was no obvious large precipitation of the Al_8Mn_5 and $Mg_{17}Al_{12}$ phases. As a result, the plasticity of the sheets with 0.9 wt.% of Y could be significantly improved, and even the elongation could reach 18%. Meanwhile, the yield strength and tensile strength still kept a relative value, i.e., 186 MPa and 271 MPa, respectively.

Author Contributions: Methodology, Y.L. and H.L.; validation, B.L., J.W., and Y.S.; formal analysis, J.W. and Z.C.; data curation, Y.S.; writing—original draft preparation, Z.C. and B.L.; writing—review and editing, J.W. and H.L. All authors have read and agreed to the published version of the manuscript.

Funding: This work was supported by the Open Fund of State Key Laboratory of Advanced Forming Technology and Equipment (SKL2020004) and the Opening Research Fund of State Key Laboratory for Advanced Metals and Materials (2021-Z08). H. X. Li thanks the National Natural Science Foundation of China (No.52171097, No.51971020) for the financial support.

Data Availability Statement: The data that support the findings of this study are available from the corresponding author, (H.X. Li.), upon reasonable request.

Conflicts of Interest: The authors declare no conflict of interest.

References

1. Jiang, B.; Yin, H.-M.; Li, R.-H.; Gao, L. Grain refinement and plastic formability of Mg-14Li-1Al alloy. *Trans. Nonferrous Met. Soc. China* **2010**, *20*, s503–s507. [[CrossRef](#)]
2. Bian, M.; Huang, X.; Mabuchi, M.; Chino, Y. Compositional optimization of Mg–Zn–Sc sheet Alloy for enhanced room temperature stretch formability. *J. Alloys Compd.* **2020**, *818*, 152891. [[CrossRef](#)]
3. Chaudry, U.M.; Kim, Y.S.; Hamad, K. Effect of Ca addition on the room-temperature formability of AZ31 magnesium alloy. *Mater. Lett.* **2019**, *238*, 305–308. [[CrossRef](#)]
4. Nakata, T.; Xu, C.; Ohashi, H.; Yoshida, Y.; Kamado, S. New Mg–Al based alloy sheet with good room-temperature stretch formability and tensile properties. *Scr. Mater.* **2020**, *180*, 16–22. [[CrossRef](#)]
5. Wu, D.; Chen, R.; Han, E. Excellent room-temperature ductility and formability of rolled Mg–Gd–Zn alloy sheets. *J. Alloys Compd.* **2011**, *509*, 2856–2863. [[CrossRef](#)]

6. Chen, J.; Zhang, Q.; Li, Q. Microstructure and mechanical properties of AZ61 magnesium Alloys with the Y and Ca combined addition. *Int. J. Met.* **2018**, *12*, 897–905.
7. Huang, X.; Suzuki, K.; Yuasa, M.; Chino, Y. Effects of initial microstructure on the microstructural evolution and stretch formability of warm rolled Mg–3Al–1Zn alloy sheets. *Mater. Sci. Eng. A* **2013**, *587*, 150–160. [[CrossRef](#)]
8. Huang, X.; Suzuki, K.; Saito, N. Enhancement of stretch formability of Mg–3Al–1Zn alloy sheet using hot rolling at high temperatures up to 823K and subsequent warm rolling. *Scr. Mater.* **2009**, *61*, 445–448. [[CrossRef](#)]
9. Tu, J.; Zhou, T.; Liu, L.; Shi, L.; Hu, L.; Song, D.; Song, B.; Yang, M.; Chen, Q.; Pan, F. Effect of rolling speeds on texture modification and mechanical properties of the AZ31 sheet by a combination of equal channel angular rolling and continuous bending at high temperature. *J. Alloys Compd.* **2018**, *768*, 598–607. [[CrossRef](#)]
10. Martynenko, N.S.; Anisimova, N.Y.; Rybalchenko, O.V.; Kiselevskiy, M.V.; Rybalchenko, G.; Straumal, B.; Temralieva, D.; Mansharipova, A.T.; Kabiyeva, A.O.; Gabdullin, M.T.; et al. Rationale for Processing of a Mg–Zn–Ca Alloy by Equal-Channel Angular Pressing for Use in Biodegradable Implants for Osteoreconstruction. *Crystals* **2021**, *11*, 1381. [[CrossRef](#)]
11. Huo, Q.; Yang, X.; Ma, J.; Sun, H.; Qin, J.; Jiang, Y. Microstructural and textural evolution of AZ61 magnesium alloy sheet during bidirectional cyclic bending. *Mater. Charact.* **2013**, *79*, 43–51. [[CrossRef](#)]
12. Shan, Z.H.; Zhang, Y.X.; Wang, B.; Zhang, Q.; Fan, J. Microstructural evolution and precipitate behavior of an AZ61 alloy plate processed with ECAP and electropulsing treatment. *J. Mater. Res. Technol.* **2022**, *19*, 382–390. [[CrossRef](#)]
13. Li, D.-W.; Wang, H.-Y.; Wei, D.-S.; Zhao, Z.-X.; Liu, Y. Effects of Deformation Texture and Grain Size on Corrosion Behavior of Mg–3Al–1Zn Alloy Sheets. *ACS Omega* **2020**, *5*, 1448–1456. [[CrossRef](#)] [[PubMed](#)]
14. Wu, Y.; Zhu, R. Effect of Rolling Temperature on the Microstructure and Mechanical Properties of AZ31 Alloy Sheet Processed through Variable-Plane Rolling. *J. Mater. Eng. Perform.* **2019**, *28*, 6182–6191. [[CrossRef](#)]
15. Wang, L.; Zhang, Z.; Cao, M.; Zhang, H.; Han, T.; Yang, Q.; Wang, H.; Cheng, W. Effect of pre-strain levels and high temperature annealing on the formability of AZ31 Mg alloy thin sheet during stretch deformation. *Mater. Res. Express* **2019**, *6*, 086595. [[CrossRef](#)]
16. Wang, Q.; Shen, Y.; Jiang, B.; Tang, A.; Chai, Y.; Song, J.; Yang, T.; Huang, G.; Pan, F. A good balance between ductility and stretch formability of dilute Mg–Sn–Y sheet at room temperature. *Mater. Sci. Eng. A* **2018**, *736*, 404–416. [[CrossRef](#)]
17. Shi, B.; Xiao, Y.; Shang, X.; Cheng, Y.; Yan, H.; Dong, Y.; Chen, A.; Fu, X.; Chen, R.; Ke, W. Achieving ultra-low planar anisotropy and high stretch formability in a Mg–1.1Zn–0.76Y–0.56Zr sheet by texture tailoring via final-pass heavy reduction rolling. *Mater. Sci. Eng. A* **2018**, *746*, 115–126. [[CrossRef](#)]
18. Chino, Y.; Huang, X.; Suzuki, K.; Sassa, K.; Mabuchi, M. Influence of Zn concentration on stretch formability at room temperature of Mg–Zn–Ce Alloy. *Mater. Sci. Eng. A* **2010**, *528*, 566–572. [[CrossRef](#)]
19. Zhao, J.; Jiang, B.; Xu, J.; He, W.; Huang, G.; Pan, F. The influence of Gd on the recrystallisation, texture and mechanical properties of Mg Alloy. *Mater. Sci. Eng. A* **2022**, *839*, 142867. [[CrossRef](#)]
20. Yin, D.; Boehlert, C.; Long, L.; Huang, G.; Zhou, H.; Zheng, J.; Wang, Q. Tension-compression asymmetry and the underlying slip/twinning activity in extruded Mg–Y sheets. *Int. J. Plast.* **2020**, *136*, 102878. [[CrossRef](#)]
21. Chen, J.K.; Chen, Y.C.; Li, H.-T.; Chan, K.-S.; Chang, C.-J. Effects of Nd and rotary forging on mechanical properties of AZ71 Mg Alloys. *Trans. Nonferrous Met. Soc. China* **2015**, *25*, 3223–3231. [[CrossRef](#)]
22. Zheng, L.W.; Zhuang, Y.P.; Li, J.-J.; Wang, H.-X.; Li, H.; Hou, H.; Wang, L.-F.; Luo, X.-P.; Shin, K.S. Mechanical properties of Mg–Gd–Zr alloy by Nd addition combined with hot extrusion. *Trans. Nonferrous Met. Soc. China* **2022**, *32*, 1866–1880. [[CrossRef](#)]
23. Silva, E.; Buzolin, R.; Marques, F.; Soldera, F.; Alfaro, U.; Pinto, H. Effect of Ce-base mischmetal addition on the microstructure and mechanical properties of hot-rolled ZK60 Alloy. *J. Magnes. Alloy.* **2021**, *9*, 995–1006. [[CrossRef](#)]
24. Liu, J.; Sun, J.; Chen, Q.; Lu, L.; Zhao, Y. Study on Microstructure and Mechanical Property in Mg–Gd–Y Alloy by Secondary Extrusion Process. *Crystals* **2021**, *11*, 939. [[CrossRef](#)]
25. Yang, W.; Quan, G.; Ji, B.; Wan, Y.; Zhou, H.; Zheng, J.; Yin, D. Effect of Y content and equal channel angular pressing on the microstructure, texture and mechanical property of extruded Mg–Y Alloys. *J. Magnes. Alloy.* **2020**, *10*, 195–208. [[CrossRef](#)]
26. Qian, X.; Zeng, Y.; Jiang, B.; Yang, Q.; Wan, Y.; Quan, G.; Pan, F. Grain refinement mechanism and improved mechanical properties in Mg–Sn alloy with trace Y addition. *J. Alloys Compd.* **2019**, *820*, 153122. [[CrossRef](#)]
27. Wang, J.H.; Wei, F.; Shi, B.; Ding, Y.; Jin, P. The effect of Y content on microstructure and tensile properties of the as-extruded Mg–1Al–xY Alloy. *Mater. Sci. Eng. A* **2019**, *765*, 138288. [[CrossRef](#)]
28. Dong, H.L.; Byoung, G.M.; Young, K.M.; Sung, H.P. Unusual relationship between extrusion temperature and tensile strength of extruded Mg–Al–Zn–Ca–Y–MM Alloy. *J. Alloys Compd.* **2021**, *862*, 158051.
29. Chaudry, U.M.; Hamad, K.; Jun, T.-S. Investigating the Microstructure, Crystallographic Texture and Mechanical Behavior of Hot-Rolled Pure Mg and Mg–2Al–1Zn–1Ca Alloy. *Crystals* **2022**, *12*, 1330. [[CrossRef](#)]
30. Chen, Y.; Zhu, Z.; Zhou, J. Study on the strengthening mechanism of rare earth yttrium on magnesium Alloys. *Mater. Sci. Eng. A* **2022**, *850*, 143513. [[CrossRef](#)]

31. Liu, X.; Wang, C.; Wen, M.; Chen, X.; Pan, F. Thermodynamic database of the phase diagrams in the Mg-Al-Zn-Y-Ce system. *Rare Met.* **2006**, *25*, 441–447. [[CrossRef](#)]
32. Fang, X.Y.; Yi, D.Q.; Wang, B.; Luo, W.-H.; Gu, W. Effect of yttrium on microstructures and mechanical properties of hot rolled AZ61 wrought magnesium Alloy. *Trans. Nonferrous Met. Soc. China* **2006**, *16*, 1053–1058. [[CrossRef](#)]